J. Membrane Biol. 150, 153–161 (1996)

The Journal of
Membrane
Biology

Functional Characterization of Canine Connexin45

E. Steiner, L. Ebihara*
Department of Pharmacology, Columbia University, New York, NY 10032

Received: 18 August 1995/Revised: 21 November 1995

Abstract. Three gap junctional proteins have been identified in canine ventricular myocytes: connexin 43 (Cx43), connexin 45 (Cx45), and connexin 40 (Cx40). We have characterized the functional properties of canine Cx45 and examined how Cx45 functionally interacts with Cx43 in *Xenopus* oocyte pairs. Homotypic pairs expressing Cx45 were well coupled. Heterotypic pairs composed of Cx45 paired with either Cx43 or Cx38 also developed high levels of conductance. Junctional currents in the heterotypic pairs displayed a highly asymmetrical voltage dependence. The kinetics and steady-state voltage dependence of the heterotypic channels more closely resembled those of the Cx45 channels when the Cx45 cRNA-injected cell was relatively negative suggesting that the Cx45 connexon closes for relative negativity at the cytoplasmic end of the channel. We also show that homotypic and heterotypic channels composed of Cx45 and Cx43 exhibit differences in pH_i sensitivity.

Key words: Intercellular communication — Connexin — Heart — Gap junction

Introduction

Propagation of electrical impulses in excitable tissues such as the heart occurs through intercellular channels which are found clustered in the form of gap junctions. In patients with healing myocardial infarcts, abnormalities in gap junctional coupling in the infarct border zones may lead to conduction abnormalities resulting in the development of reentrant ventricular tachycardias and sudden cardiac death (Luke & Saffitz, 1991; Spach & Dolber, 1986; Ursell et al., 1985). Gap junctions are also thought to mediate the exchange of metabolites and signal molecules between neighboring cells and to be involved in the regulation of cardiac growth and development (Reaume et al., 1995; Loewenstein & Rose, 1992; Paul et al., 1995).

Gap junctional channels are formed from a family of closely related proteins called connexins. At least twelve different types of mammalian connexins have been recently identified including 3 connexins which are present in the dog heart: connexin43 (Cx43), connexin40 (Cx40) and connexin45 (Cx45) (Kanter, Saffitz, & Beyer, 1992). Each of these connexins exhibits a distinct spatial and temporal distribution. Cx43 is the predominant gap junctional protein in the working myocardium while Cx40 is found at highest levels in the conduction system (Kanter et al., 1993*a*). Cx45 has been detected in adult canine ventricular myocytes where it colocalizes with Cx43 and Cx40 (Kanter, Saffitz, & Beyer, 1992; Kanter et al., 1993*b*). Cx45 is also expressed in a number of mammalian cell lines including SkHep1, WB, BHK, A7r5, CLEM and BWEM cells (Laing et al., 1994), in the chick heart (Beyer, 1990), in many tissues from the adult and embryonic mouse (Butterweck et al., 1994) and in neonatal rat heart cells.

Although it has been shown that Cx43, Cx45 and Cx40 can colocalize to the same gap junctional plaque, it is not clear whether the 3 connexins can localize to the same intercellular channel. There are two different ways that intercellular channels composed of multiple connexins could form. The connexons or hemichannels could be hetero-oligomers containing more than one type of connexin or two connexons composed of different connexins could join to form a heterotypic intercellular channel.

In the present study, we have examined how Cx45 and Cx43 functionally interact using the paired *Xenopus* oocyte expression system (Dahl et al., 1987). We show

* *Present address:* Department of Physiology and Biophysics, Finch University of Health Sciences/The Chicago Medical School, 3333 Green Bay Road, North Chicago, Il 60064

Correspondence to: L. Ebihara

that Cx45 can form homotypic intercellular channels with itself and heterotypic channels with Cx43. The homotypic and heterotypic intercellular channels exhibit differences in sensitivity to transjunctional voltage and cytoplasmic acidification.

Materials and Methods

In vitro Transcription

The canine Cx45 clone was a generous gift from Dr. Eric Beyer (Washington University, St. Louis, MO). The DNA for Cx45 was subcloned into the Eco RI of the RNA expression vector, SP64TII, between the 5′ and 3′ noncoding regions of *Xenopus* β-hemoglobin. SP64TII was constructed as previously described (Ebihara, Berthoud, & Beyer, 1995).

Plasmids containing the entire coding region of Cx45, Cx43 and Cx38 were linearized with an appropriate restriction enzyme and transcribed in vitro using SP6 RNA polymerase (Promega Corporation, Madison, WI). The methylated RNA cap analogue, 5′m^{7}G(5′)ppp(5′)G (New England Biolabs, Beverly, MN), was added to the transcription buffer to produce capped RNAs. The transcripts were purified on a spun column to remove unincorporated rNTPs and precipitated with ethanol. The transcripts were then resuspended in DEPC-treated water and aliquots were stored at –80°C. The quality and amount of cRNA was assessed visually using formaldehyde gel electrophoresis.

Preparation of Oocytes

Xenopus oocytes were prepared as previously described (Ebihara & Steiner, 1993). The oocytes were injected with 40 nl of an oligonucleotide, antisense to mRNA for *Xenopus* Cx38, 24 hr prior to injection with cRNA. This treatment was previously shown to drastically reduce endogenous coupling (Barrio et al., 1991; Bruzzone et al., 1993; Hennemann et al., 1992). The oocytes were injected with cRNA, devitellinized and paired as previously described (Ebihara & Steiner, 1993) except that in some of the experiments, the vitelline membrane was removed chemically by incubating the oocytes in acid MBS (pH = 2.5) for several minutes on a rocker.

Immunoprecipitation

The affinity purified antibody against Cx45 (amino acids 285–298) used in the immunoprecipitation studies was a gift of Dr. Eric Beyer (Washington University, St. Louis). The specificity of this antibody has been previously demonstrated by immunofluorescence and by immunoprecipitation of in vitro translated connexins (Kanter et al., 1993*b*).

Defolliculated *Xenopus* oocytes were coinjected with connexin cRNA and S^{35}-methionine and incubated overnight at 18°C. The labeled oocytes were homogenized in 300 μl/oocyte lysis buffer (in mM: 20 Tris, H 7.5, 100 NaCl, 2 EDTA supplemented with 10 NEM and 2 PMSF) by passage through an 18-gauge needle. The homogenate was precleared by centrifugation in a microfuge at 8,000 rpm, 4°C for 10 min to pellet yolk granules. The supernatant was supplemented with 200 μM leupetin and 0.6% SDS, boiled for 3 min and then passed 3 times through a 26-gauge needle. The samples were diluted with four volumes of ''immunoprecipitation buffer'' (in mM: 0.1 NaCl, 0.02 Na borate, 15 EDTA, 0.02% Na azide, 10 NEM and 2 PMSF, pH 8.5 supplemented with 0.5% Triton X-100 and affinity purified antiserum to Cx45) and incubated overnight at 4°C with 20 μl/oocyte Protein A beads (Sigma Chemical, St. Louis, MO). The Protein A beads were then collected by gentle centrifugation for 3 min and washed four times with ''immunoprecipitation buffer'' supplemented with .5% Triton X-100, .5% BSA and 1% SDS, solubilized in SDS sample buffer at 100°C for 5 min and analyzed by SDS-PAGE.

Electrophysiological Measurements

Junctional conductance was measured using a dual two microelectrode voltage clamp technique (Spray, Harris & Bennett, 1981). The microelectrodes were filled with a solution containing 1.5 M KCl, 10 mM EGTA and 10 mM Hepes, pH 7.4 and had resistances of .5 – 2 MΩ. To prevent KCl from leaking into the oocyte, the tips of the electrodes were filled with agar. Voltage clamping was performed using two Axoclamp 2A amplifiers (Axon Instruments, Foster City, CA). The experiments were controlled and data were collected with an analog-to-digital (A-D) converter system (TL-1 DMA interface, 100 kHz, Axon Instruments, Foster City, CA) and PClamp6 software (Axon Instruments). The current signal was filtered at 20 Hz using a four-pole Bessel filter. Analysis and graphical presentation of the data were done with PClamp6 (Axon Instruments) and Fig P (Biosoft, Cambridge, UK) software. Both cells of a pair were initially held at a holding potential of –40 mV. To measure junctional conductance, a voltage-clamp step was applied to one cell while the other member of the pair was held at –40 mV. The change in current required to hold the cell at –40 mV during the voltage-clamp step was equal to the current flowing through the gap junction. Only oocyte pairs with junctional conductances less than 10 μsec were selected for analysis of voltage-dependent behavior in order to avoid errors due to series resistance or access resistance.

Results

Immunoprecipitation

The ability of Cx45 cRNA to direct the synthesis of Cx45 protein in *Xenopus* oocytes was examined by coinjecting oocytes with Cx45 cRNA and [^{35}S]methionine. Lysates of metabolically labeled oocytes were immunoprecipitated using an affinity-purified antibody directed against Cx45. The immunoprecipitated protein was electrophoresed on a 12% SDS-polyacrylamide gel and analyzed by fluorography (Fig. 1). A major protein with a M_r of ~45 kDa was detected in Cx45 cRNA-injected oocytes. This protein had an electrophoretic mobility similar to the in vitro translated product. No electrophoretic bands were detected in water-injected oocytes.

Functional Expression of Cx45

The *Xenopus* oocyte pair system was used to investigate whether Cx45 could form homotypic intercellular channels with itself or heterotypic channels with Cx43. Oocytes were pretreated with DNA oligonucleotides antisense to *Xenopus* connexin38 mRNA, injected with Cx45 or Cx43 cRNA and paired. Homotypic Cx45/Cx45 and heterotypic Cx43/Cx45 pairs formed intercellular channels (Table 1). We also showed that Cx45

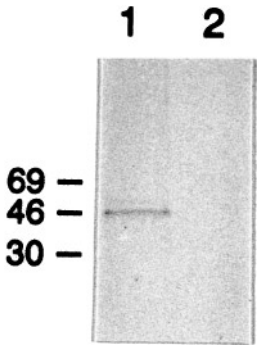

Fig. 1. Immunoprecipitation of connexin45 from oocytes metabolically labeled with [^{35}S]methionine. Homogenates prepared from Cx45 cRNA- (lane 1) or water-injected (lane 2) oocytes were processed for immune precipitation, separated on a 12% SDS-polyacrylamide gel and detected by fluorography. Migration of protein standards are indicated at the left edge of the gel.

Table 1. Cx45 forms homotypic channels with itself and heterotypic channels with Cx43 and Cx38

Oocyte injection cell 1/cell 2	Junctional conductance (μS)[a]	No. of pairs[b]
Cx45/Cx45	4.37 ± 2.33	5
Cx45/Cx43	2.99 ± 2.25	4
Cx45/Cx38	6.9 ± 4.28	3

[a] Values are mean ± SD.
[b] Only the low conductance pairs used to analyze the voltage dependence are included.

could form heterotypic intercellular channels with the endogenous *Xenopus* embryonic gap junctional protein, *Xenopus* connexin38 (Cx38), by pairing Cx45 cRNA-injected oocytes with noninjected control oocytes or oocytes injected with the cRNA for Cx38 (Table 1). To test whether the gap junctional conductances recorded in heterotypic Cx43/Cx45 pairs were due entirely to the expression of exogenous connexins, we compared coupling levels in antisense/Cx45 and Cx43/Cx45 oocyte pairs (Table 2). Our results showed that the Cx43/Cx45 pairs exhibited much higher levels of coupling than the antisense/Cx45 pairs suggesting that pretreatment with antisense Cx38 oligonucleotides prevented the formation of heterotypic channels between Cx45 and endogenous Cx38. Untreated control pairs exhibited low but variable levels of coupling.

Voltage Gating of Cx45 Homotypic Channels

Figure 2*A* shows a typical family of junctional current traces recorded from an oocyte pair injected with Cx45 cRNA. The junctional currents decayed to a new steady-state level on application of depolarizing and hyperpolarizing transjunctional voltage-clamp steps. The relationship between transjunctional potential, V_j, and initial (G_{jo}, solid circles) and steady-state ($G_{j\infty}$, open squares) junctional conductance is shown in Fig. 2*B*. Both G_{jo} and $G_{j\infty}$ were normalized in each cell pair to the value of G_j at 0 mV. $G_{j\infty}$ decreased symmetrically at positive and negative V_js. This behavior was quantitated by fitting the $G_{j\infty}$-V_j relationship to a Boltzmann equation (Table 3). Steady-state parameters previously determined for homotypic channels composed of Cx43 or Cx38 have also been included in Table 3 for comparison. In con-

Table 2. Junctional conductance in Cx45/Cx43 pairs is not due to the recruitment of endogenous connexin by Cx45

Oocyte injection cell 1/cell 2	G_j (range) μS[a]	No. of pairs[c]
Cx45/Cx43	6.96 ± 7.99 (0–14.7)	4
Cx45/antisense	.0147 ± .036 (0–.09)	6
Control/control[b]	1.34 ± 1.4 (0–2.8)	3

[a] Values are mean ± SD.
[b] Control pairs were not pretreated with antisense Cx38 oligonucleotide.
[c] To reduce variability in levels of endogenous and exogenous connexins, all of the experiments were performed on oocytes from a single donor frog.

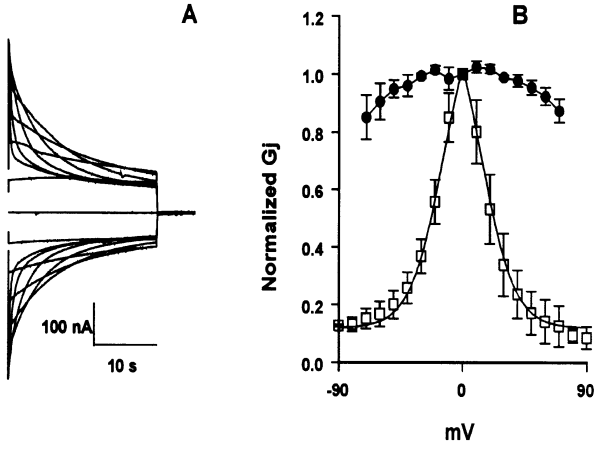

Fig. 2. Oocyte pairs expressing Cx45 exhibit characteristic voltage-dependent behavior. (*A*) Representative gap junctional current traces recorded from a homotypic Cx45 oocyte pair. Gap junctional current traces were generated by applying transjunctional voltage clamp steps to ±90 mV in 10 mV increments from a holding potential of –40 mV. (*B*) Plot of the mean initial (filled circles) and steady-state (open squares) junctional conductance *vs.* transjunctional voltage relation. The steady-state junctional conductance was determined at $T = 24$ sec. The initial junctional conductance was determined by fitting the time course of decay of the junctional current to a double exponential and extrapolating to $T = 0$ sec. Smooth lines are the best fit of the experimental data to a Boltzmann function whose parameters are given in Table 3. Results are shown as means ± SEM of 5 oocyte pairs whose mean conductance is given in Table 1.

Table 3. Boltzmann parameters for homotypic channels expressed in *Xenopus* oocytes[a]

Cx (Condition)[b]	A	z	V_o (mV)	G_{jmax}	G_{jmin}
Cx45	0.084	2.1	14	1.3	0.115
Cx43 (+V_j)[c]	0.07	1.8	55	1.0	0.18
Cx43 (–V_j)[c]	0.09	2.2	–59	1.0	0.40
Cx38[d]	0.20	5.0	25	1.0	0.29

[a] Data were fit to a Boltzmann equation of the form $G_{j\infty} = (1 - G_{jmin})/(1 + \exp(A(V - V_o))) + G_{jmin}$. The cooperativity constant A can also be expressed in terms of equivalent number of gating charges z.
[b] $\pm V_j$ refers to the polarity of the transjunctional potential. If not indicated the response was symmetrical.
[c] Cx43 data are from White et al. (1994).
[d] Cx38 data are from Bruzzone et al. (1994). The recording solution used in these experiments were identical to that used in the present experiments.

trast to Cx43, Cx45 homotypic channels displayed a much greater sensitivity to transjunctional voltage with V_o (the voltage at which G_j was reduced by 50%) of ±14 mV and G_{jmin} (the value of the minimum conductance for large transjunctional voltages) of .115. G_{jo} decreased gradually for increasing potentials of either polarity.

The time course of inactivation of the gap junctional current could be described by a monoexponential process for $V_j \leqslant \pm 50$ mV as illustrated in Fig. 3*A*. At larger potentials, the decay process was best fit by the sum of two exponentials. The rate of decay was strongly voltage dependent becoming faster with increasing V_j. The mean time constant of inactivation, τ, determined from 4 experiments was plotted as a function of V_j in Fig. 3*B*. τ decreased by a factor of ~4 between 10 and 50 mV.

The time course of recovery of the gap junctional conductance was measured using a double pulse protocol (Fig. 3*C*). During the first depolarizing step, G_j decayed to a new steady-state level. Following a recovery period of variable duration, a second test depolarizing pulse was applied to measure the fraction of junctional channels that had recovered from inactivation. As illustrated in Fig. 3*C*, the time course of recovery was best fit by an exponential process with a time constant, τ, of 5.7 sec.

Experiments on amphibian blastomere pairs (Spray, Harris & Bennett, 1981) indicated that gap junctional channels closed by a transjunctional voltage of one polarity must reopen before they can be closed by a voltage of the opposite polarity. To test whether Cx45 channels behave in a similar manner, a 60 mV transjunctional voltage-clamp pulse was applied in the absence and presence of a prepulse of the opposite polarity as illustrated in Fig. 3*D*. When the test pulse was given alone, the junctional current decayed monophasically to a new steady-state value. When the test pulse was preceeded by a prepulse, the junctional current increased before declining and the rate of decay was much slower. In contrast to the difference in time course, the area under current trace remained constant. These findings support the notion that the channel must retrace its steps, passing back to the open state before the other gate can close.

Voltage Gating of Heterotypic Channels

Figure 4 shows typical families of transjunctional currents and plots of the normalized junctional conductance (G_j) *vs.* transjunctional voltage (V_j) relationship for the heterotypic oocyte pairs. Junctional currents in the heterotypic Cx43/Cx45 pairs displayed a highly asymmetrical voltage dependence (Fig. 4*A*). When a hyperpolarizing voltage-clamp step was applied to the Cx45 cRNA-injected cell, the junctional current inactivated to a steady-state level. The rate of closure increased with increasing transjunctional voltage. In contrast, depolarization of the cell expressing Cx45 evoked junctional currents that slowly increased with time. For large depolarizations, the junctional current rose to a peak value within seconds and then slowly inactivated. The current did not reach steady state during pulses as long as 48 sec. To compare the slow voltage dependence of the heterotypic channels to the parent connexins, the normalized junctional conductance at $T = 24$ sec was plotted as a function of V_j. The conductance measured at $T = 24$ sec ($G_{j\infty}$, open squares) reached a maximum value at $V_j \sim 25$ mV and decayed asymmetrically at more positive and negative potentials with V_o (the voltage at which G_j was reduced by 50%) ~60 mV for positive V_js and ~–5 mV for negative V_js. Although the voltage sensitivities were altered compared to the parent connexins, the time course of decay and the steady-state voltage dependence of the heterotypic channels more closely resembled those of the homotypic Cx45 channels when the Cx45 cRNA-injected cell was relatively negative suggesting that the Cx45 connexon closes for relative negativity at the cytoplasmic end of the channel.

To better understand the extent to which the voltage-dependent behavior of connexons composed of Cx45 or Cx43 are influenced by the molecular composition of the opposing connexon, we also characterized the voltage-dependent properties of heterotypic gap junctional channels composed of Cx38 and Cx45 or Cx43 (Fig. 4*B* and *C*). Heterotypic Cx38/Cx45 channels closed for relative negativity and opened for relative positivity of the Cx45 cell. For large depolarizing pulses applied to the Cx45 cell, G_j exhibited a biphasic response consisting of an initial increase followed by a slower decline to a lower steady-state value. These properties were similar to those of the Cx43/Cx45 heterotypic channels. There were subtle differences in kinetics and initial and steady-state G_j-V_j curves. Heterotypic channels composed of Cx38 and Cx45 showed a less pronounced reduction in G_{jo} and $G_{j\infty}$ for large positive potentials applied to the

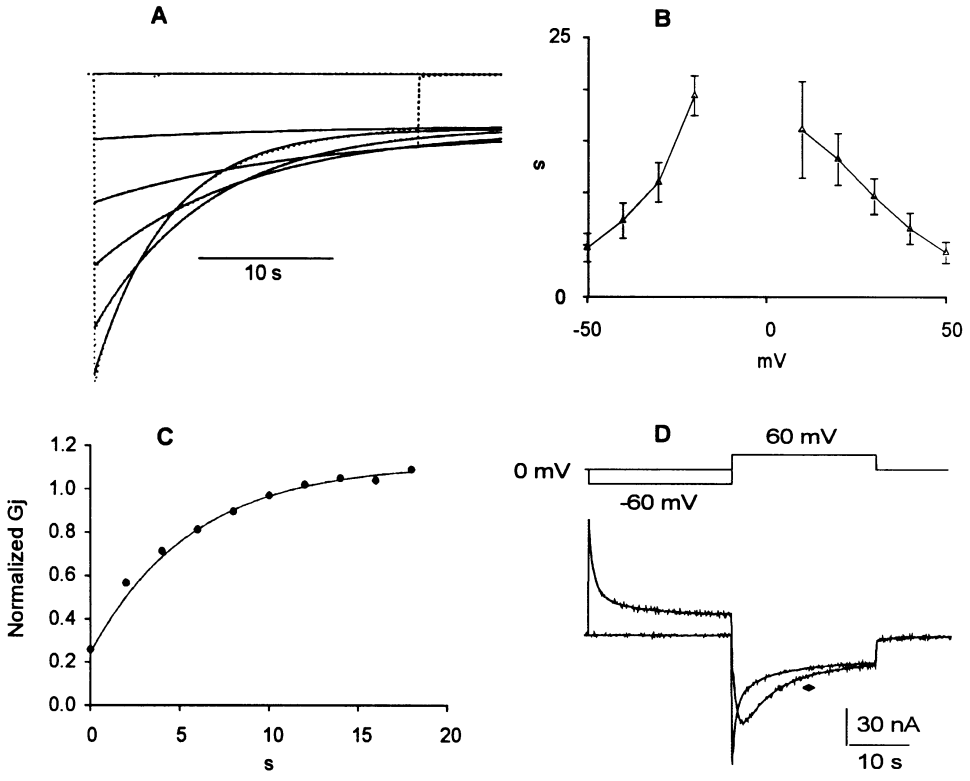

Fig. 3. Kinetics of inactivation and recovery from inactivation. (*A*) Time course of inactivation of the Cx45 junctional current during 24-sec pulses to potentials between 10 and 50 mV. The unbroken lines represent a monoexponential fit to the data. (*B*) Time constant of inactivation plotted as a function of transjunctional potential. Data are shown as means ± SEM of 4 oocyte pairs. (*C*) Time course of recovery of the gap junctional conductance following a large transjunctional voltage clamp pulse. The time course of recovery of the Cx45 gap junctional current was measured using a double pulse protocol. The peak junctional current measured during the second pulse (normalized with respect to the peak junctional current recorded during the first pulse) was plotted as a function of interpulse interval. (*D*) Effect of polarity reversal. Junctional currents were determined during a 60 mV pulse when given alone and when preceded by a prepulse of opposite polarity (closed diamond). When the pulse is preceded by a prepulse of opposite polarity which reduces the junctional conductance, the current transiently increases and then decreases.

Cx45 cell and a smaller residual $G_{j\infty}$ for large negative potentials.

Heterotypic channels composed of Cx38 and Cx43 also showed highly asymmetrical steady-state voltage sensitivities (Fig. 4*C*). G_j decayed to a steady-state level of about 10% of its initial value for large negative potentials applied to the Cx43-injected cell and 66% of its initial value for large positive potentials. Unlike the Cx38/Cx45 and Cx43/Cx45 heterotypic channels, G_j decayed with a monophasic time course in response to depolarizing voltage-clamp steps applied to the Cx43 cell.

pH_i Sensitivity

To examine the effect of cytoplasmic acidification on junctional conductance, oocyte pairs were superfused with MBS equilibrated with 100% CO_2 at a constant flow rate of 5 ml/min. When homotypic Cx43 and Cx45 pairs were superfused with MBS equilibrated with 100% CO_2, they showed an initial increase in junctional conductance followed by a decrease as illustrated in Fig. 5*A*. The rate and extent of the decline differed. Cell pairs expressing Cx45 (open squares) uncoupled with a faster time course and to a greater extent than Cx43/Cx43 pairs (filled circles). This effect was reversible on washout. Similar results were obtained in 4 other experiments. In contrast, homotypic Cx38 pairs (filled stars) showed only a reduction in G_j. The time course of decay of G_j was more rapid than that observed for the Cx43 or Cx45 pairs.

Heterotypic pairs were also sensitive to cytoplasmic acidification. Heterotypic channels formed from Cx45 and Cx38 could be distinguished from Cx43/Cx45 channels by their increased susceptibility to acidification-induced uncoupling. Figure 5*B* compares results obtained from a Cx38/Cx45 pair (open circles) with those recorded from a Cx43/Cx45 pair (filled circles). Cx38/Cx45 channels closed more rapidly and recovered much more slowly upon removal of CO_2 than Cx43/Cx45 channels.

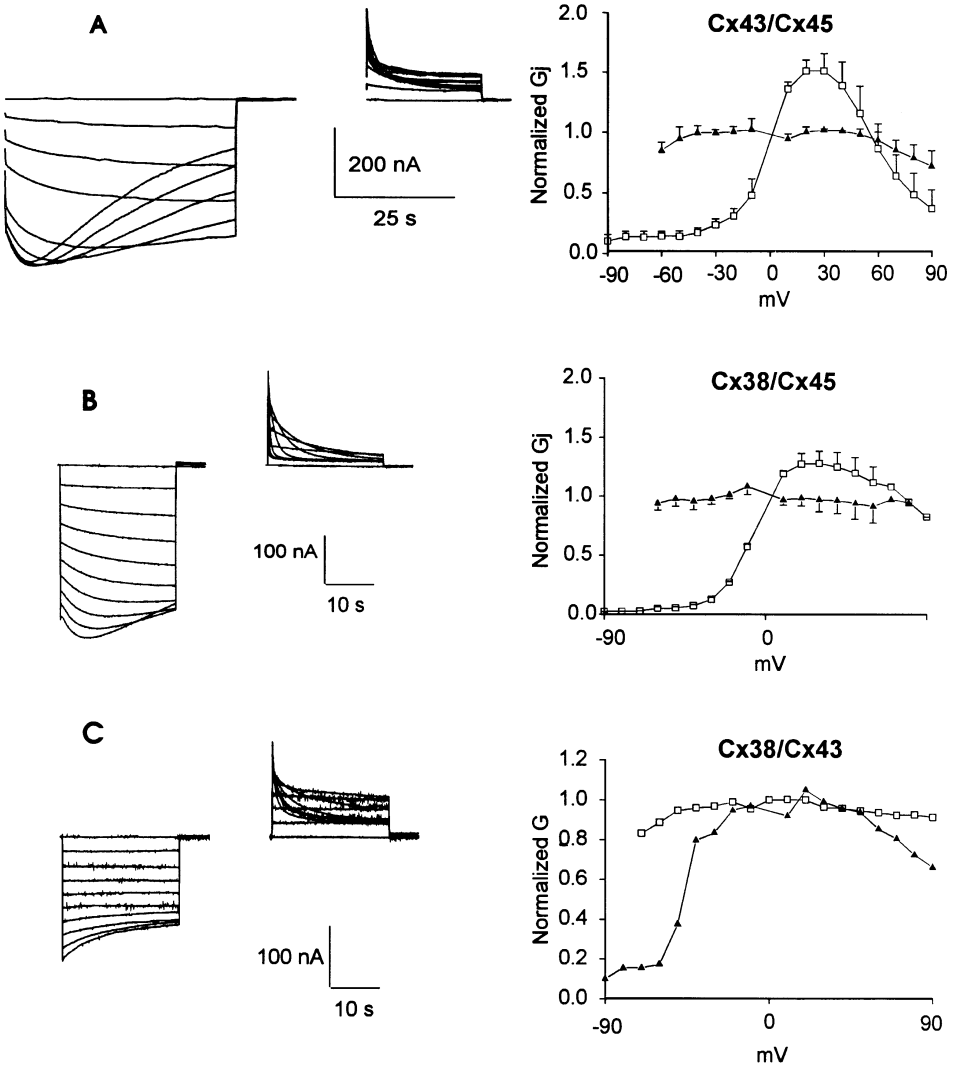

Fig. 4. Heterotypic channels exhibit highly asymmetrical voltage-dependent behavior. Oocyte pairs were initially voltage clamped to a holding potential of −40 mV and then 24-sec voltage clamp steps were applied in increments of 10 mV between −90 and 90 mV to cell 2. Junctional current was measured in cell 1 and thus was negative when cell 2 was depolarized and positive when cell 2 was hyperpolarized. Transjunctional potentials were always measured relative to cell 2. The initial and steady-state conductance were measured at $T = 30$ msec and 24 sec, respectively and normalized to their value at 0 mV. Typical junctional current traces and plots of the mean initial (filled triangles) and steady-state (open squares) conductance *vs.* transjunctional voltage are presented for Cx43/Cx45 (*A*), Cx38/Cx45 (*B*) and Cx38/Cx43 (*C*) pairs. Data are shown as means ± SEM of 4 oocyte pairs for Cx45/Cx43 and 3 oocyte pairs for Cx45/Cx38 whose mean conductances are given in Table 1.

Discussion

To explore how the molecular diversity of gap junctional proteins influences intercellular communication in the heart, we have examined the functional interactions of 2 mammalian cardiac gap junctional proteins (canine Cx45 and rat Cx43) in paired *Xenopus* oocytes. Our results show that Cx45 could form homotypic intercellular channels with itself and heterotypic channels with Cx43. The homotypic Cx45 channels were strongly voltage dependent. Their voltage-gating properties resemble those of chicken Cx45, a gap junctional protein found in many tissues from the chicken embryo whose amino acid sequence is 83% identical to that of mammalian Cx45 (Veenstra et al., 1992; Barrio et al., 1995).

Polarity reversal experiments suggest that Cx45 gap junctional channels closed by transjunctional voltages of one polarity must open before they could be closed by a voltage of the opposite polarity. Similar behavior has been observed for gap junctional channels between amphibial blastomeres (Spray, Harris, & Bennett, 1981), rat schwann cells (Chanson et al., 1993) and cells from an

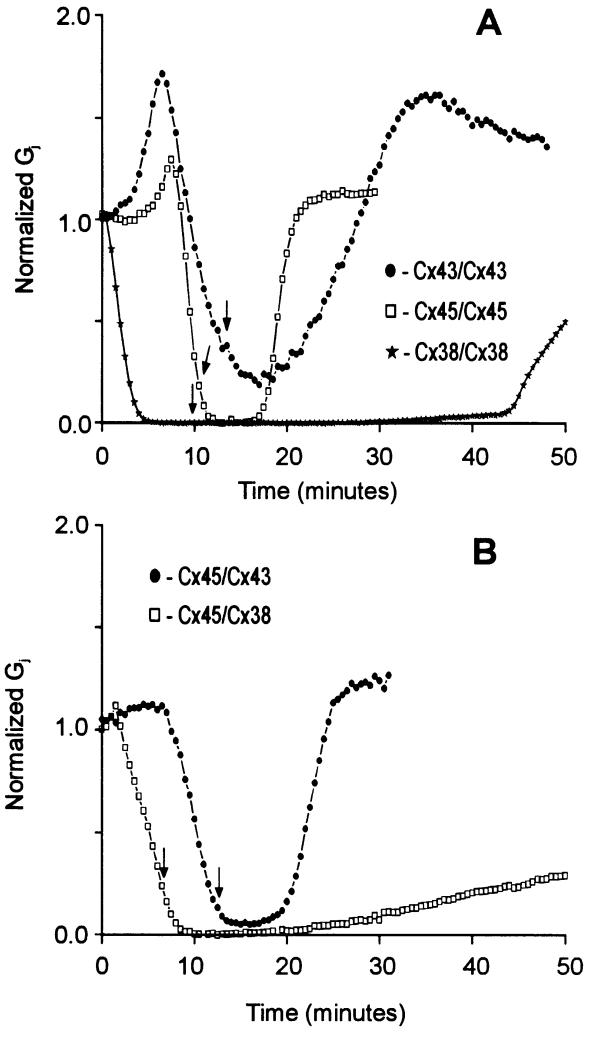

Fig. 5. Effect of cytoplasmic acidification. Oocyte pairs were initially superfused with normal MBS at a constant flow rate of 5 ml/min (total bath volume ~5 ml). At $T = 0$ the perfusion solution was switched to MBS equilibriated with 100% CO_2 for ~10 mins and then switched back to normal MBS (arrow). G_j was measured by applying 5 mV depolarizing transjunctional voltage-clamp pulses for 400 msec at 30-sec intervals. The holding potential was −40 mV. G_j was normalized to its value determined immediately before switching to 100% CO_2 and plotted as a functional of time for representative homotypic (*A*) and heterotypic (*B*) cell pairs composed of Cx45, Cx43 or Cx38.

insect cell line (Bukauskas & Weingart, 1994). To account for this behavior, Spray et al. (1981) proposed that each hemichannel has a gate which senses local voltage drops within the channel and that when one gate is closed, the entire transjunctional voltage gradient occurs across that gate. When the polarity of the voltage is reversed, the closed gate must open before the other gate can sense the voltage gradient. Alternatively, closure of one gate might physically interfere with the other gate closing.

Comparison of the voltage-dependent properties of heterotypic Cx43/Cx45 and Cx38/Cx45 channels with those of the parent connexins indicate that both the kinetic properties and the steady-state voltage dependence of heterotypic channels more closely resemble those of the homotypic Cx45 channels when hyperpolarizing pulses were applied to the cell expressing Cx45. However, the residual conductance at large transjunctional potentials is lower when Cx45 is paired with Cx38. This observation suggests that the behavior of the Cx45 hemichannel is modified by the molecular composition of the opposing connexon.

The behavior of the heterotypic channels was more complex for depolarizing pulses applied to the Cx45-injected cell. Depolarization elicited a transient increase in the junctional current followed by a slow decline. The activating component had a time course similar to the time course of recovery of the homotypic Cx45 channels. These observations could be explained if it is assumed that both hemichannels close for relative negativity and that the Cx45 hemichannel is only partially activated at 0 mV. Under these conditions, the contingency model (Spray, Harris & Bennett, 1981) predicts that when a depolarizing pulse is applied to the Cx45 cell, channels with the Cx45 gate closed must open before the other gate can close resulting in an increase in junctional conductance followed by a decrease. Similar findings for heterotypic gap junction channels formed from human Cx45 and Cx43 expressed in SKHep1 cells have been recently reported in preliminary form by Moreno et al. (1995).

It was originally proposed that hemichannels close on depolarization of the cell containing the hemichannels and this was supported by the observation that in heterotypic Cx43/Cx38 oocyte pairs, G_j was strongly reduced by depolarization of the Cx38-containing cell but not by potentials of the opposite polarity (Swenson et al., 1989; Werner et al., 1989). In exception to this generalization, Cx32, Cx46 and Cx56 were recently reported to close on hyperpolarization of the connexin-containing cell (Verselis, Ginter & Bargiello, 1994; Paul et al., 1991; Ebihara & Steiner, 1993; Ebihara, Berthoud & Beyer, 1995). In the present study, we were able to clearly demonstrate that Cx45 closes for relative negativity of the Cx45-injected cell because of the unique voltage-dependent properties of Cx45. Moreover, our data suggest that Cx43 may also close for relative negativity. It is interesting to note that although the kinetics of inactivation of the Cx43 hemichannel in heterotypic Cx43/Cx45 pairs are markedly slower than the kinetics of inactivation of the Cx43 hemichannel in heterotypic Cx43/Cx38 pairs, the steady-state voltage-dependent properties of the heterotypic Cx43/Cx45 channels resemble those of the Cx43/Cx38 channels for relative negativity of the Cx43-injected cell.

Gap junctional conductance can also be modulated by intracellular pH. The specific degree of pH_i sensitiv-

ity varies in different tissues (Spray & Bennett, 1985). This variation could reflect differences in connexin expression, post-translational processing or intracellular environment. It has been recently shown that homotypic Cx43 and Cx32 channels exhibit different sensitivities to pH_i when expressed in oocytes (Liu et al., 1993). Furthermore, the pH_i sensitivities of Cx43 and Cx32 in oocytes closely resemble those observed in cardiac ventricular myocytes (White et al., 1990) and hepatocyte cell pairs (Spray et al., 1986), respectively. These findings suggest that the difference in pH_i sensitivity between liver and cardiac gap junctions is due to differences in structural features of their connexins. In the present study, we have used the oocyte pair system to characterize and compare the pH_i sensitivity of homotypic and heterotypic channels composed of Cx45 and Cx43. Our results show that both the homotypic and heterotypic channels are sensitive to pH_i. The homotypic Cx45 and Cx43 channels show clear differences in the rate and extent of acid-induced uncoupling suggesting that they are not being modulated by pH_i in the same way. It is interesting to speculate that differences in distribution of Cx45, Cx43 and Cx40 in cardiac tissues may lead to differences in the susceptibility of these tissues to acid-induced uncoupling during myocardial ischemia.

This study was supported by National Institutes of Health grant HL-45377, a Grant-in-Aid from the New York City Affiliate of the American Heart Association, and an Irma Hirschl Career Scientist Award.

References

Barrio, E.C., Jarillo, J.A., Beyer, E.C., Saez, J.C. 1995. Comparison of voltage dependence of chick connexin 42 and 45 channels expressed in pairs of *Xenopus* oocytes. *In:* Intercellular Communication through Gap Junctions. Y. Kanno, K. Kataoka, Y. Shiba, Y. Shibata, and T. Shimazu, editors. pp.391–394. Elsevier, Amsterdam

Barrio, L.C., Suchyna, T., Bargiello, T., Xu, L.X., Roginsky, R., Bennett, M.V.L., Nicholson, B.J. 1991. Voltage dependence of homo- and hetero-typic cx26 and cx32 gap junctions expressed in *Xenopus* oocytes. *Proc. Natl. Acad. Sci. USA* **88:**8410–8414

Beyer, E.C. 1990. Molecular cloning and developmental expression of two chick embryo gap junction proteins. *J. Biol. Chem.* **265:**14439–14443

Bruzzone, R., Haeffliger, J.-A., Gimlich, R.L., Paul, D.L. 1993. Connexin40, a component of gap junctions in vascular endothelium, is restricted in its ability to interact with other connexins. *Molecular Biology of the Cell* **4:**7–20

Bruzzone, R., White, T.W., Paul, D.L. 1994. Expression of chimeric connexins reveals new properties of the formation and gating behavior of gap junction channels. *J. Cell Sci.* **107:**955–967

Bukauskas, F.F., Weingart, R. 1994. Voltage-dependent gating of single gap junction channels in an insect cell line. *Biophys. J.* **67:**613–625

Butterweck, A., Gergs, U., Elfgang, C., Willecke, K., Traub, O. 1994. Immunochemical characterization of the gap junction protein connexin45 in mouse kidney and transfected human HeLa cells. *J. Membrane Biol.* **141:**247–256

Chanson, M., Chandross, K.J., Rook, M.B., Kessler, J.A., Spray, D.C. 1993. Gating characteristics of a steeply voltage-dependent gap junction channel in rat schwann cells. *J. Gen. Physiol.* **102:**925–946

Dahl, G., Miller, T., Paul, D.L., Voellmy, R., Werner, R. 1987. Expression of functional cell-cell channels from cloned rat liver gap junction complementary cDNA. *Science* **236:**1290–1293

Ebihara, L., Berthoud, V.M., Beyer, E.C. 1995. Distinct behavior of connexin56 and connexin46 gap junctional channels can be predicted from the behavior of their hemi-gap-junctional channels. *Biophys. J.* **68:**1796–1803

Ebihara, L., Steiner, E. 1993. Properties of a nonjunctional currents expressed from a rat connexin46 cDNA in Xenopus oocytes. *J. Gen. Physiol.* **102:**59–74

Hennemann, H., Suchyna, T., Lichtenberg-Frate, H., Jungbluth, S., Dahl, E., Schwarz, H.-J., Nicholson, B.J., Willecke, K. 1992. Molecular cloning and functional expression of mouse connexin40, a second gap junction gene preferentially expressed in lung. *J. Cell Biol.* **117:**1299–1310

Kanter, H.L., Beyer, E.C., Laing, J.G., Beau, S.L., Saffitz, J.E. 1993*a*. Distinct patterns of connexin expression in canine Purkinje fibers and ventricular muscle. *Circ. Res.* **72:**1124–1131

Kanter, H.L., Laing, J.G., Beyer, E.C., Green, K.G., Saffitz, J.E. 1993*b*. Multiple connexins colocalize in canine ventricular myocyte gap junctions. *Circ. Res.* **73:**344–350

Kanter, H.L., Saffitz, J.E., Beyer, E.C. 1992. Cardiac myocytes express multiple gap junction proteins. *Circ. Res.* **70:**438–444

Laing, J.G., Westphale, E.M., Engelmann, G.L., Beyer, E.C. 1994. Characterization of the gap junction protein, connexin43. *J. Membrane Biol.* **139:**31–40

Liu, S., Taffet, S., Stoner, L., Delmar, M., Vallano, M.L., Jalife, J. 1993. A structural basis for the unequal sensitivity of the major cardiac and liver gap junctions to intracellular acidification: the carboxyl tail length. *Biophys J.* **64:**1422–1433

Loewenstein, W.R., Rose, B. 1992. The cell-cell channel in the control of growth. *Semin. Cell Biology* **3:**59–79

Luke, R.A., Saffitz, J.E. 1991. Remodeling of ventricular conduction pathways in healed canine infarct border zones. *J. Clin. Invest.* **87:**1597–1602

Moreno, A.P., Fishman, G.I., Beyer, E.C., Spray, D.C. 1995. Voltage dependent gating and single channel analysis of heterotypic gap junction channels formed of Cx45 and Cx43. *In:* Intercellular Communication through Gap Junctions. Y Kanno, K. Kataoka, Y. Shiba, Y. Shibata, and T. Shimazu, editors. pp.405–408. Elsevier, Amsterdam

Paul, D.L., Ebihara, L., Takemoto, L.J., Swenson, K.I., Goodenough, D.A. 1991. Connexin46, a novel lens gap junction protein, induces voltage-gated currents in nonjunctional plasma membrane of *Xenopus* oocytes. *J. Cell Biol.* **115:**1077–1089

Paul, D.L., Yu, K., Bruzzone, R., Gimlich, R.L., Goodenough, D.A. 1995. Expression of a dominant negative inhibitor of intercellular communication in the early *Xenopus* embryo causes delamination and extrusion of cells. *Development* **121:**371–381

Reaume, A.G., de Sousa, P.A., Kulkarni, S., Langille, B.L., Zhu, D., Davies, T.C., Juneja, S.C., Kidder, G.M., Rossant, J. 1995. Cardiac malformation in neonatal mice lacking connexin43. *Science* **267:**1831–1834

Spach, M.S., Dolber, P.C. 1986. Relating extracellular potentials and their derivatives to anisotropic propagation at a microscopic level in human cardiac muscle: evidence for electrical uncoupling of side-to-side fiber connections with increasing age. *Circ. Res.* **58:**356–371

Spray, D.C., Ginzberg, R.D., Morales, E.A., Gatmitan, Z., Arias, I.M. 1986. Electrophysiological properties of gap junctions between dissociated pairs of rat hepatocytes. *J. Cell Biol.* **103:**135–144

Spray, D.C., Bennett, M.V.L. 1985. Physiology and pharmacology of gap junctions. *Annu. Rev. Physiol.* **47:**281–303

Spray, D.C., Harris, A.L., Bennett, M.V.L. 1981. Equilibrium properties of voltage dependent junctional conductance. *J. Gen. Physiol.* **77:**77–93

Swenson, K.I., Jordan, J.R., Beyer, E.C., Paul, D.L. 1989. Formation of gap junctions by expression of connexins in *Xenopus* oocyte pairs. *Cell* **57:**145–155

Ursell, P.C., Gardner, P.I., Albala, A., Fenoglio, J.J.J., Wit, A.L. 1985. Structural and electrophysiological changes in the epicardial border zone of canine myocardial infarcts during infarct healing. *Circ. Res.* **56:**436–451

Veenstra, R.D., Wang, H., Westphale, E.M., Beyer, E.C. 1992. Multiple connexins confer distinct regulatory and conductance properties in the developing heart. *Circ. Res.* **71:**1277–1283

Verselis, V.K., Ginter, C.S., Bargiello, T.A. 1994. Opposite voltage gating polarities of two closely related connexins. *Nature* **368:**348–351

Werner, R., Levine, E., Rabadan-Diehl, C., Dahl, G. 1989. Formation of hybrid cell-cell channels. *Proc. Natl. Acad. Sci. USA* **86:**5380–5384

White, R.L., Doeller, J.E., Verselis, V.K., Wittenberg, B.A. 1990. Gap junctional conductance between pairs of ventricular myocytes is modulated synergistically by H^+ and Ca^{++}. *J. Gen. Physiol.* **95:**1061–1075